Functional brain connectome and its relation to Hoehn and Yahr stage in Parkinson's disease

Xueling Suo[1*] MM, Du Lei [1,2*] PhD, Nannan Li[3] MD, Lan Cheng[3] MD, Fuqin Chen[4] MD, Meiyun Wang[5] MD PhD, Graham J Kemp[6] MA DM, Rong Peng[3] MD PhD, Qiyong Gong[1] MD PhD

Author Affiliations:

1. Huaxi MR Research Center, Department of Radiology, West China Hospital, Sichuan University, Chengdu Sichuan, 610041 China
2. Department of Psychosis Studies, Institute of Psychiatry, Psychology & Neuroscience, King's College London, London, SE5 8AF United Kingdom
3. Department of Neurology, West China Hospital, Sichuan University, Chengdu Sichuan, 610041 China
4. Department of Medical Information Engineering, School of Electrical Engineering and Information, Sichuan University, Chengdu Sichuan, 610065 China
5. Department of Radiology, Henan Provincial People's Hospital & the People's Hospital of Zhengzhou University, Zhengzhou Henan, 450003 China
6. Department of Musculoskeletal Biology and MRC-Arthritis Research UK Centre for Integrated Research into Musculoskeletal Ageing (CIMA), Faculty of Health and Life Sciences, University of Liverpool, Liverpool, L69 3GE United Kingdom

*Xueling Suo and Du Lei contributed to this work equally.

Correspondence to: Prof. Qiyong Gong

Address: Huaxi MR Research Center, Department of Radiology, West China Hospital, Sichuan University, No. 37 Guo Xue Xiang, Chengdu, Sichuan 610041, China.

E-mail: qiyonggong@hmrrc.org.cn; **Tel**: 086-028 81812593; **Fax**: 086-028 85423503

Funding and disclosure information:

This study was supported by the National Natural Science Foundation (Grant Nos. 81621003, 81220108013 and 81501452), the Program for Changjiang Scholars and Innovative Research Team in University (PCSIRT, grant IRT1272) of China, the Changjiang Scholar Professorship Award (Award No. T2014190) of China, and the CMB Distinguished a Professorship Award (Award No. F510000/ G16916411) administered by the Institute of International Education. D.L. supported by Newton International Fellowship from the Royal Society. The authors declare no competing financial interests.

Note: This paper has not been presented at an RSNA meeting or accepted for presentation at a future meeting.

Type of manuscript being submitted: original research

Word count for the text: 2934

Functional brain connectome and its relation to Hoehn and Yahr stage in Parkinson's disease

Manuscript type: Original research

Advances in Knowledge

1. In resting-state functional magnetic resonance imaging studies of patients with Parkinson's disease (PD), we observed lower values of clustering coefficient Cp (P=0.0002), local efficiency Eloc (P=0.0006) and global efficiency Eglob (P=0.0002) and higher values of characteristic path length Lp (P=0.0006) relative to healthy controls (HC), indicating that the functional connectome in PD patients is perturbed.

2. We observed decreased nodal centralities (P<0.001, false discovery rate corrected) in the sensorimotor cortex, temporal-occipital regions and default mode network.

3. The nodal centralities in the right precentral gyrus, left postcentral gyrus (PoCG) and left superior temporal gyrus (STG) decreased with increasing Hoehn and Yahr stage in the patients (P< 0.05, with one-way analysis of variance).

4. The scores of Unified PD Rating Scale-III were negatively correlated with the nodal degree of the left PoCG (P=0.038, FDR corrected, r=-0.198) and nodal efficiency of left STG (P=0.009, FDR corrected, r=-0.270).

Implication for Patient Care

In this study we demonstrated a decrease in the nodal centralities in the right precentral gyrus, left postcentral gyrus and left superior temporal gyrus in PD patients that is related to clinical symptom severity as judged by Hoehn and Yahr stage. The findings suggest that the resting-state functional connectome reflects neural functional changes in relation to disease severity in PD patients, and therefore might serve as a biomarker of disease progression.

Summary statement

Using resting-state functional magnetic resonance imaging with graph analysis to investigate topological organization of the brain in PD in relation to disease severity, the decrease in nodal centralities with increasing Hoehn and Yahr stage was restricted to the sensorimotor and temporal cortex.

ABSTRACT

Purpose: To use resting-state functional magnetic resonance imaging (rs-fMRI) and graph theory approaches to investigate the brain functional connectome and its potential relation to disease severity in Parkinson's disease (PD).

Materials and Methods: This case-control study was approved by the local research ethics committee, and all subjects provided informed consent. We recruited 153 right-handed PD patients and 81 healthy controls (HC) matched for age, gender and handedness to undergo a 3T rs-fMRI scan. The whole brain functional connectome was constructed by thresholding the partial correlation matrices of 90 brain regions, and the topological properties were analyzed using graph theory approaches. We used nonparametric permutation tests to compare topological properties, and then assessed their relationship to disease severity.

Results: The functional connectome in PD showed abnormalities at the global level (decrease in clustering coefficient Cp, global efficiency Eglob, and local efficiency Eloc, and increase in characteristic path length Lp) and at the nodal level (decreased nodal centralities in the sensorimotor cortex, default mode and temporal-occipital regions) ($P < 0.001$, FDR corrected). Furthermore, the nodal centralities in left postcentral gyrus and left superior temporal gyrus correlated negatively with Unified PD Rating Scale-III score ($P=0.038$, FDR corrected, $r=-0.198$; $P=0.009$, FDR corrected, $r=-0.270$, respectively), and decreased with increasing Hoehn and Yahr stage in PD.

Conclusion: The configurations of brain functional connectome in PD patients were perturbed and correlated with disease severity, notably those responsible for motor functions. These results provide topological insights into understanding the neural functional changes in relation to disease severity of PD.

INTRODUCTION

Parkinson's disease (PD), a common degenerative disorder of the central nervous system, is characterized by cardinal motor symptoms and nonmotor dysfunctions (1). While the pathological process is mainly attributed to disruptions in the nigrostriatal dopamine system, it also involves more widespread cerebral cortical areas (2). Neuroimaging research suggests that some progressive impairment in PD might reflect alterations in distributed brain networks (3). There are no effective non-invasive biomarkers to assess PD progression.

Functional neuroimaging research increasingly focuses on integrated brain function rather than individual brain areas. Resting-state functional magnetic resonance imaging (rs-fMRI), which reflects baseline neuronal brain activity, can be used to detect interregional correlations in blood oxygen level dependent (BOLD) signal fluctuations, permitting study of intrinsic large-scale brain network organization with potential relevance for the diagnosis and assessment of neurodegenerative diseases (4).

Recent advances in graph-based network theory allow the direct noninvasive characterization of brain network topology (5). For graph-theoretical analysis of neural networks using rs-fMRI, anatomical brain regions are considered as nodes, linked by edges, which represent the connectivity measured by the temporal correlation of BOLD signal fluctuations between the nodes (6). Networks which display a balance between integration and segregation are considered 'small-world' networks, characterized by high clustering and low path length, allowing fast information transfer with reduced energy expenditure (6). This approach has been used to study the brain structural and functional connectome in healthy subjects and in psychiatric and neurological diseases such as depression (7) and PD (8-11). However, findings in PD have been inconsistent (8-10). Furthermore, these studies

have mainly focused on early and mid-stage patients (8, 10), and could therefore not identify progressive brain changes over different stages.

Thus the present study aims to use rs-fMRI and graph theory approaches to investigate the brain functional connectome and its potential relation to disease severity in PD.

MATERIALS AND METHODS

This case-control study was approved by the local ethics committee, and written informed consent was obtained from all subjects (or their legal guardians) prior to enrollment.

Participants

Study participants were consecutively recruited at the movement disorders outpatient clinic of West China Hospital of Sichuan University from September 2013 to January 2016. We recruited 170 right-handed patients with a diagnosis of PD made by clinical neurologists (L.C., N.L. and R.P.; 5, 6 and 30 years, respectively, of clinical neurology experience) according to the clinical diagnostic criteria of the UK Parkinson's Disease Society (12). The Unified PD Rating Scale (UPDRS) -III was used to assess motor disability (13), and Hoehn and Yahr stage (HY stages 1–5) to evaluate disease severity (14). Mini-Mental State Exam (MMSE) was used to evaluate cognition (15). The patients had been either drug-naïve at the initial visit or unmedicated for at least 12 hours before participation. In view of the practical difficulties of performing MRI studies in patients at HY stage 5 (wheelchair-bound or bedridden unless assisted), we recruited only HY stage 1-4 patients. See Appendix for details of exclusion criteria and MMSE evaluation. Finally, 153 patients (67 male; 86 female) were included in the study.

In addition, 81 right-handed age- and gender-matched healthy controls (HC) (36 male; 45 female) were recruited from the local area by poster advertisements, and assessed by neurologists (L.C., N.L.; 5 and 6 years, respectively, of clinical neurology experience). HC were excluded if they had any neurological illness, as assessed by clinical evaluation and medical records, or structural brain defects on T1- or T2-weighted images.

Data acquisition and pre-processing

All subjects had an rs-fMRI scan using a 3T Siemens Trio Tim magnetic resonance system (Siemens Healthineers, Erlangen, Germany) equipped with a 12-channel phased array head coil. See Appendix for full sequence parameters. Each functional scan contained 240 image volumes, resulting in a total scan time of 480 s. Participants were instructed not to focus their thoughts on anything in particular and to keep their eyes closed during the acquisition. Head motion was minimized using foam pads. Conventional MRI protocols were performed with a fast spin-echo sequence for the structural assessment: axial T1-weighted, T2-weighted and fluid-attenuated inversion recovery images were obtained. Two neuroradiologists (X.S., M.W.; 4 and 18 years, respectively, of neuroradiological MRI experience) verified image quality and evaluated for clinical abnormalities.

SPM8 (http://www.fil.ion.ucl.ac.uk/spm) was used to perform image preprocessing, as described in Appendix. In brief the steps are: removal of the first 10 time points; slice timing correction; realignment; spatial normalization; time-course de-trending and band-pass filtering (0.01-0.08 Hz); and nuisance signal regression (16).

Construction of functional connectome

The network was constructed using GRETNA (http://www.nitrc.org/projects/gretna/) (17). A network is composed of nodes and edges between nodes. First, the whole brain was divided into 90 cortical and subcortical regions of interest using the automated anatomical labeling (AAL) atlas with each representing a network node. Next, to define the edges of the network, we acquired the mean time series of each region, and calculated the partial correlations of the mean time series between all pairs of nodes (representing their conditional dependences by excluding the effects of the other 88 regions) (7). This resulted in a 90 × 90 partial correlation matrix for each subject, which was converted into a binary matrix according to a predefined threshold (see below for the threshold selection), where the entry aij = 1 if the absolute partial correlation between regions i and j exceeds threshold, and aij= 0 otherwise (7).

Global brain analysis

We applied a sparsity threshold S to all correlation matrices (see Appendix). For the brain networks at each sparsity level, we calculated both global and nodal network metrics and then the area under the curve (AUC) over the sparsity range (Figure S2). The global metrics were of two kinds: small-world parameters [for definitions see (18)] including the clustering coefficient Cp, characteristic path length Lp, normalized clustering coefficient γ, normalized characteristic path length λ, and small-worldness σ; and network efficiency parameters [for definitions see (19)] including the local efficiency Eloc and global efficiency Eglob. The nodal centrality metrics were the nodal degree (6), nodal efficiency (20), and nodal betweenness (7).

To locate the specific pairs of brain regions with altered functional connectivity in PD, we identified region pairs that exhibited between-group differences in nodal characteristics and then used the network-based statistics (NBS) method (http://www.nitrc.org/projects/nbs/) (21) to define a set of suprathreshold significant changes between any connected regions ($P < 0.05$, threshold, $T = 0.572$) (7). Statistical significance was estimated using the nonparametric permutation method (10,000 permutations).

Statistical Analysis

The analyses of demographic and clinical data were performed in SPSS 16.0 software (http://www.spss.com). Two-tailed independent-sample t test, one-way analysis of variance (ANOVA), and chi-squared test were used to compare quantitative and qualitative variables, respectively. To compare the network properties of the functional connectomes between PD and HC, we used nonparametric permutation tests in Matlab (www.mathworks.com) (22) to identify significant between-group differences in the AUCs of all the network metrics, as described previously (7, 23, 24). To address the problem of multiple comparisons of nodal centralities, we adopted a Benjamini Hochberg False Discovery Rate (FDR) correction method at a significance level of 0.001 (25). After significant between-group differences were identified in the network metrics, we extracted the AUC values of topological properties in each region showing significant difference. Comparison among the different HY stage patients and HC was performed using ANOVA, followed by post hoc two-sample t tests. Finally, partial correlations were computed to examine relationships between these values and UPDRS-III and MMSE scores in PD with education as covariate.

RESULTS

Demographic and Clinical Comparisons

We report demographic and clinical data from 153 PD and 81 HC summarized in Table 1. Age and gender did not differ significantly between the PD and HC group ($P > 0.05$). The mean years of education in the HC group were higher than the PD group's ($P = 0.003$). There were significant differences in disease duration ($P < 0.001$), UPDRS-III score ($P < 0.001$), age at onset ($P = 0.04$) and levodopa equivalent daily dose (LEDD) ($P < 0.001$) among different HY stage PD.

Global topological organization of the functional connectome

In the defined threshold range, both PD and HC showed small-world topology in the brain functional connectome. Compared with HC, PD showed a significant decrease in the clustering coefficient Cp ($P = 0.0002$), global efficiency Eglob ($P = 0.0002$) and local efficiency Eloc ($P = 0.0006$), and an increase in the characteristic path length Lp ($P = 0.0006$) (Figure 1, Table E1), with no significant differences in normalized clustering coefficient γ ($P = 0.5807$), normalized characteristic path length λ ($P = 0.0098$) or small-worldness σ ($P = 0.9122$).

Regional topological organization of the functional connectome

We identified the brain regions showing significant between-group differences in at least one nodal metric ($P < 0.001$, FDR corrected). Compared with HC, PD showed decreased nodal centralities in the right precentral gyrus (PreCG), right Rolandic operculum, right posterior cingulate gyrus (PCG), right fusiform gyrus, right supramarginal gyrus (SMG), bilateral postcentral gyrus (PoCG), left superior frontal gyrus (SFG), left angular gyrus (ANG), left Heschl gyrus, bilateral superior temporal gyrus (STG) (Figure 2, Table 2). There were no increased nodal centralities.

PD-related alterations in functional connectivity

The NBS method identified a significantly altered network in PD. This network had 12 nodes and 28 connections (Figure 2), mainly involved in sensorimotor cortex, default mode network (DMN) and temporal-occipital regions. Within this network, all of the connections were decreased in PD compared with HC.

Correlation analysis

Based on this between-group difference in topological organization, a decrease in the nodal centralities in the right PreCG, left PoCG and left STG with increasing HY stage were found (Figure 3), which were all connected with right PCG, left SFG and left ANG (Figure 2, Table 3). Furthermore, UPDRS-III score was negatively correlated with nodal degree of the left PoCG ($P=0.038$, FDR corrected, $r=-0.198$) and nodal efficiency of left STG ($P=0.009$, FDR corrected, $r=-0.270$) (Figure 4).

DISCUSSION

This study investigated the topological properties of the functional connectome in a relatively large cohort (n=153) of PD patients of HY stages 1-4, compared to HC. PD showed abnormalities at the global level (a decrease in the clustering coefficient Cp, global efficiency Eglob, and local efficiency Eloc, and an increase in the characteristic path length Lp) and at the nodal level (decreased nodal centralities in the sensorimotor cortex, DMN and temporal-occipital regions). Furthermore, some of these abnormalities were related to measures of clinical severity: a decrease in the nodal centralities

in the right PreCG, left PoCG and left STG, which were correlated to a higher HY stage, were observed in DMN regions, including right PCG, left SFG and left ANG; moreover, the nodal degree of the left PoCG and nodal efficiency of left STG were negatively correlated with UPDRS-III score. These findings may provide insights into the neurobiology of PD, and aid development of new biomarkers of disease progression.

In the framework of graph theory, a network is declared as 'small world' when it attains a balance between local specialization (indexed by a high clustering coefficient Cp) and global integration (indexed by low characteristic path length Lp) (26). In the present study the brain networks of both PD and HC exhibited small-worldness. However, the networks in PD were perturbed in a way that may reflect the underlying pathophysiology. In regard to global topologies, Cp, Eglob and Eloc were decreased while Lp was increased in PD compared to HC, suggesting that the networks in PD were less locally specialized and less globally integrated. These results are consistent with recent structural and functional connectome studies (27, 28) in which brain networks of early-to-mid clinical stage PD showed decreased local specialization and global integration. However, others report decreased local specialization (indicated by decreased Cp and Eloc) and maintained global integration in the brain functional network of early-stage PD (8). A longitudinal magnetoencephalography (MEG) study with graph analysis showed a progressive impairment in local specialization with an additional loss of global integration in PD (29). In the light of our results, these studies suggest that as the disease progresses brain networks in PD may eventually fail to maintain global integration.

Besides these altered global topologies, PD showed impaired nodal centralities of several regions in the functional connectome, including the sensorimotor cortices, temporal-occipital regions and DMN. Decreased nodal centralities in the sensorimotor cortex accord with the classical motor impairment of PD. Abnormalities in white matter integrity and specific functional network alterations have been reported in PD (30, 31). Unlike those studies, we did not find any significant changes in the basal ganglia, perhaps surprisingly given that the basal ganglia motor circuits are critical in motor deficits in PD. Possible explanations may be found in our study design. The heterogeneity of selected patients and modalities of connectivity measurement might contribute to the difference. Besides, although medication was withdrawn in treated PD at least 12 hours prior to rs-fMRI scanning, we cannot completely rule out the potentially confounding effects of chronic dopaminergic drugs, which may have obscured alterations in the basal ganglia. Furthermore, previous neuroimaging studies in PD have focused on the basal ganglia using a seed-point method. By examining predefined regions of interest, some important cerebral alterations may have been missed. The temporal-occipital regions are important for visual object recognition, and decreased nodal centralities in these regions have been observed before in PD (8), associated with impaired bottom-up visual processing (32). The relevance of the DMN for cognitive processes (33) has been reinforced by recent evidence in neurodegenerative disorders such as Alzheimer's disease (AD) (34). Our DMN findings are compatible with the suggested role for dysfunctional DMN connectivity in the development of cognitive decline in PD (35).

The decrease in nodal centralities with disease progression was restricted to right PreCG, left PoCG and left STG, all connected with DMN regions, suggesting that distributed brain regions might affect the functional interaction of brain networks. A cross-sectional rs-fMRI analysis reported decreased functional connectivity involving left temporal cortex as disease progress (36). A 4-year longitudinal MEG study in PD found that abnormalities of functional connectivity evolved to include increasingly widespread brain regions in close relation to clinical (both motor and cognitive) deterioration (37). That study was restricted to early clinical disease in order to track progressive brain changes. Our cross-sectional study included a wider range of clinical stages of PD, which can provide insights into disease progression without the confounding influence of time. Our results are consistent with the MEG study's finding of early abnormalities in temporal cortex (37), and extend this in two ways: the decreased nodal centralities in temporal cortex begin in the early and mid-stage, and become more prominent in the advanced stage; and with disease progression, decreased nodal centralities appear

in the sensorimotor cortex. Our observation of decreased nodal centralities in the temporal and sensorimotor cortices is congruent with neuropathological observations that Lewy body pathology invades the cortex through these same regions in Braak stage 4 and 5 (38). Moreover, there were significant negative correlations between UPDRS-III scores and nodal centralities of the left PoCG and left STG. In accordance with our results, published fMRI studies report an inverse correlation between the voxel-mirrored homotopic connectivity of sensorimotor, regional homogeneity of temporal cortex and UPDRS-III score in PD (3, 39). Sensorimotor dysfunction contributes crucially to motor difficulties in PD. Interestingly, increased motor-speech impairment scores are reportedly associated with decreased connectivity involving STG (40). The nodal centralities of the left PoCG and left STG might be a potential biomarker for motor progressive impairment in PD. Overall, the present study provides further evidence that changes in resting functional brain networks can reflect neural functional changes in relation to disease severity in PD, and therefore serve as a potential biomarker for disease progression.

Our study has several limitations that need to be taken into account when interpreting the data. First, no detailed cognitive testing such as the cognitive scale- Montreal cognitive assessment (MoCA) was performed and MMSE scores were only acquired in the patient group, which could confound our conclusions. Our results need to be confirmed in future studies with a comprehensive assessment of cognitive function. Second, the choice of network nodes has been somewhat arbitrary across published studies. We used the AAL atlas to parcellate the entire brain into 90 regions, but differences in template parcellations may cause considerable variations in graph-based theoretical parameters, which must be explicitly compared in future work. Third, physiological noise, including respiratory and cardiac fluctuations, might have compromised our results. Fourth, further studies will be needed to quantify potential differences between drug-naive and treated PD cohorts to evaluate the effect of the medication on topological properties of brain networks. Fifth, the correlation coefficients between the UPDRS-III and nodal centralities of left PoCG, and left STG were quite low, so this correlation analysis should be considered exploratory. Sixth, to avoid the confounding effects of age we enrolled patients with similar age, but there may be confounding factors such as years of education, which will need to be addressed in future studies.

In summary, we used rs-fMRI and graph-theoretical approaches to investigate the topology of the brain functional connectome and possible disease severity-related alterations in PD patients. We found PD patients had topologic functional disorganizations of brain networks, as evidenced by less local specialization and less global integration relative to HC. Nodal centralities were reduced mainly in the sensorimotor cortex, DMN and temporal-occipital regions of PD, consistent with the motor changes in these patients. The decrease in nodal centralities with increasing HY stage was restricted to the sensorimotor and temporal cortex, and was negatively correlated with the UPDRS-III score. These results may provide insights into the underlying neurobiology of PD, and aid development of new biomarkers of disease progression in PD.

Appendix

Materials and Methods

In the current study, we define abnormal MMSE in our patients: ≤ 17 for illiterate subjects, ≤ 20 for grade-school literate, and ≤ 23 for junior high school and higher education literate (41). Patients were excluded if they had liver and kidney disease, drug/alcohol abuse, or cerebrovascular disorders including previous stroke, a history of head injury, seizure, hydrocephalus, intracranial mass, neurological surgeries, or other neurologic disease, any disorder that interfered with the assessment of PD (e.g. essential tremor and dystonic tremor), or excessive head motion during scanning (translational movement >1.5 mm and/or rotation >1.5°). Seventeen patients were excluded for the following reasons: 3 patients for contraindication to MRI; 4 patients with radiologically observed cerebrovascular disease with cortical or subcortical infarct(s) or white matter lesions on structural MRI evaluation by two neuroradiologists (X.S., M.W.; 4 and 18 years, respectively, of neuroradiological MRI experience); 4 patients for image distortion; 6 patients for excessive head motion. Finally, 153 patients (67 male; 86 female) were included in the study (Figure S1).

MR Image Acquisition

The following sequences were performed as follows: 1) rs-fMRI: repetition time/echo time (TR/TE) = 2000/30 ms, flip angle = 90°, 30 axial slices per volume, 5 mm slice thickness (no slice gap), matrix = 64 × 64, FOV = 240 × 240 mm^2, voxel size = 3.75 × 3.75 × 5 mm^3; 2) T1-weighted imaging: TR/TE = 1600/9.2 ms, flip angle = 130°, 21 axial slices, 5 mm slice thickness, matrix = 148 × 320, FOV = 250 × 250 mm^2, voxel size = 1.2 × 0.8 × 5.0 mm^3; 3) T2-weighted imaging: TR/TE = 4000/93 ms, flip angle = 120°, 21 axial slices, 5 mm slice thickness, matrix = 230 × 320, FOV = 220 × 220 mm^2, voxel size = 0.8 × 0.7 × 5.0 mm^3; 4) fluid-attenuated inversion recovery imaging: TR/TE = 6000/93 ms, flip angle = 130°, 21 axial slices, 5 mm slice thickness, matrix = 198 × 256, FOV = 220 × 220 mm^2, voxel size = 1.0 × 0.9 × 5.0 mm^3.

MR Image Analysis

MR image analysis was performed by two authors (X. S., D. L.; 4 and 9 years of experience in neuroimaging, respectively).The first 10 time points were discarded to avoid instability of the initial MRI signal. Then, the images were corrected for intra-volume acquisition time delay and inter-volume geometric displacement of head motion. After these corrections, the images were spatially normalized to a 3 × 3 × 3 mm^3 Montreal Neurological Institute (MNI) 152 template and then linearly detrended and temporally bandpass filtered (0.01-0.08 Hz) to remove low-frequency drift and high-frequency physiological noise. Finally the global signal, the white matter signal, the cerebrospinal fluid (CSF) signal and the motion parameters (1.5 translational and 1.5 rotational parameters) were regressed out (16).

Global brain analysis

To address the problem that networks of individual subjects differed in the number of edges (42), we applied a range of sparsity thresholds, S, to the correlation matrices to provide each graph with the same number of edges, thereby enabling us to investigate between group differences in relative network organization (7). The S procedure has been described in detail in previous publications, generating a threshold range of $0.10 < S < 0.34$ with an interval of 0.01 (23,24). This thresholding strategy produced networks that could estimate small-worldness with sparse properties and the minimum number of spurious edges (18). For each network metric we calculated the area under the curve (AUC) over the sparsity range from S_1 to S_n with an interval of ΔS, where $S_1 = 0.10$, $S_n = 0.34$ and $\Delta S = 0.01$ (Figure S2). The AUC provides a summarized scalar for the topological characterization of brain networks that is independent of a single threshold selection and sensitive to topological alterations in brain disorders (7).

Table E1. The different AUC values of global properties in the brain functional connectome between PD patients and HC.

Global properties	PD	HC	P*
Eglobal (Global efficiency)	0.070±0.004 (0.060-0.080)	0.072±0.004 (0.064-0.081)	0.0002
Elocal (Local efficiency)	0.094±0.009 (0.075-0.118)	0.099±0.010 (0.076-0.119)	0.0006
Cp (Clustering coefficient)	0.070±0.010 (0.050-0.096)	0.075±0.011 (0.052-0.099)	0.0002
Lp (Characteristic path length)	0.827±0.048 (0.725-0.954)	0.803±0.044 (0.723-0.907)	0.0006

Measurements presented as mean±SD with ranges in parentheses.
*P < 0.001, nonparametric permutation tests.
Abbreviations: PD, Parkinson's disease; HC, healthy control.

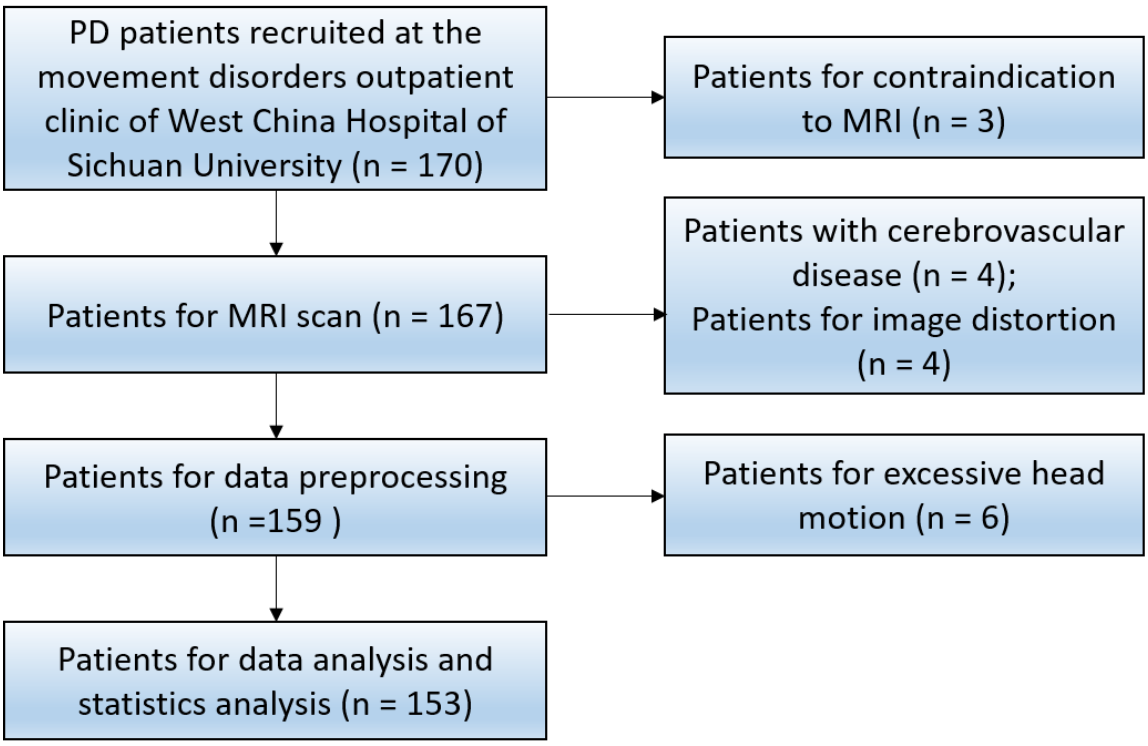

Figure S1. Flowchart for the PD patients' recruitment.

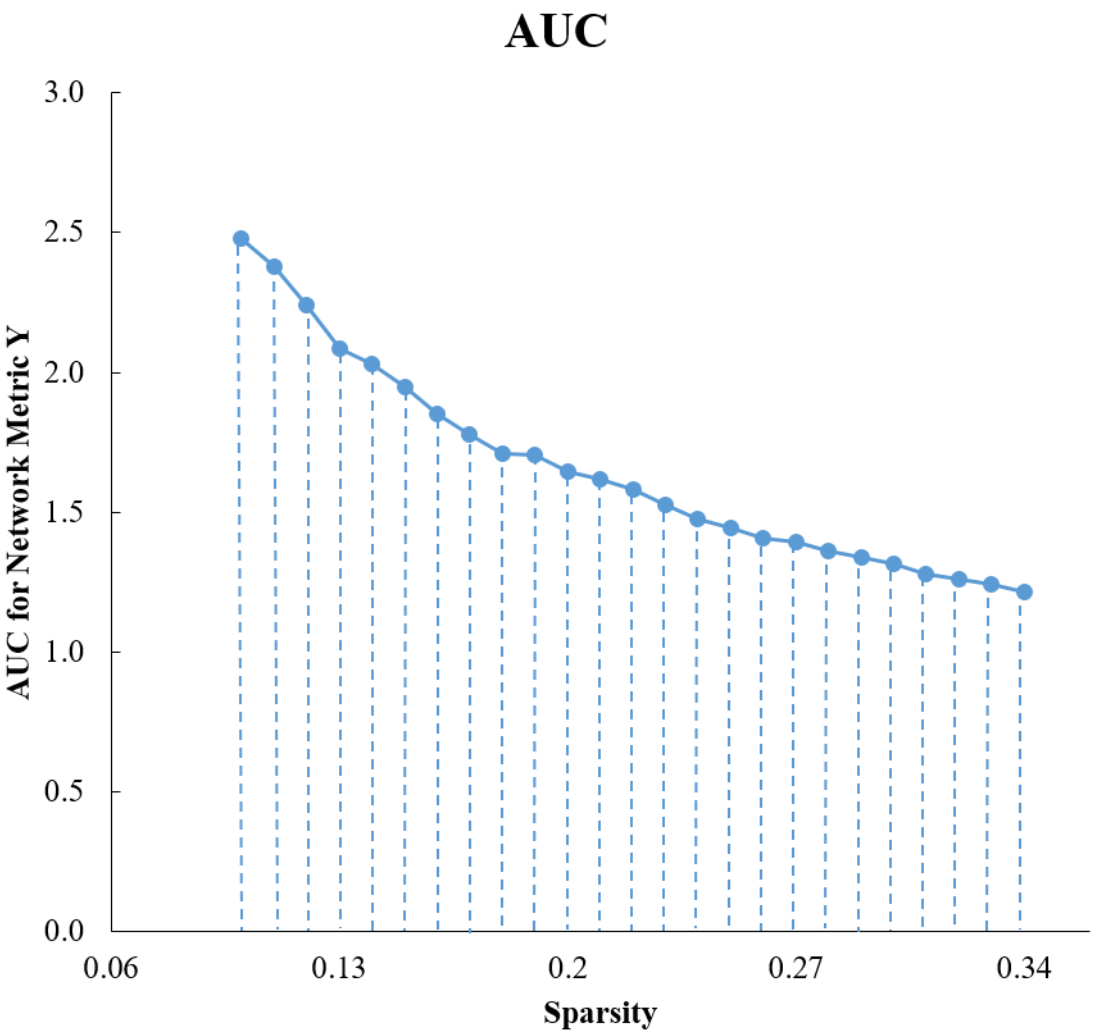

Figure S2. The illustration of area under curve (AUC) for network metrics. The AUC for a network metric Y which was calculated over the sparsity threshold range of S_1 to S_n with interval of ΔS, was computed as $Y^{AUC} = \sum_{k=1}^{n-1}[Y(S_k) + Y(S_{k+1})] \cdot \Delta S/2$. In the current study, S_1= 0.10, S_n = 0.34 and ΔS = 0.01.

References for Appendix

41. Luo C, Song W, Chen Q, et al. Reduced functional connectivity in early-stage drug-naive Parkinson's disease: a resting-state fMRI study. Neurobiol Aging. 2014;35(2):431-41.
42. Wen W, Zhu W, He Y, et al. Discrete neuroanatomical networks are associated with specific cognitive abilities in old age. J Neurosci. 2011;31(4):1204-12.

REFERENCES

1. Jankovic J. Parkinson's disease: clinical features and diagnosis. J Neurol Neurosurg Psychiatry. 2008;79(4):368-76.

2. Zhang J, Bi W, Zhang Y, et al. Abnormal functional connectivity density in Parkinson's disease. Behav Brain Res. 2015;280:113-8.

3. Luo C, Guo X, Song W, et al. Decreased Resting-State Interhemispheric Functional Connectivity in Parkinson's Disease. Biomed Res Int. 2015;2015:692684.

4. Fox MD, Raichle ME. Spontaneous fluctuations in brain activity observed with functional magnetic resonance imaging. Nat Rev Neurosci. 2007;8(9):700.

5. Bullmore E, Sporns O. Complex brain networks: graph theoretical analysis of structural and functional systems. Nat Rev Neurosci. 2009;10(3):186-98.

6. Rubinov M, Sporns O. Complex network measures of brain connectivity: uses and interpretations. Neuroimage. 2010;52(3):1059-69.

7. Zhang J, Wang J, Wu Q, et al. Disrupted brain connectivity networks in drug-naive, first-episode major depressive disorder. Biol Psychiatry. 2011;70(4):334-42.

8. Luo CY, Guo XY, Song W, et al. Functional connectome assessed using graph theory in drug-naive Parkinson's disease. J Neurol. 2015;262(6):1557-67.

9. Gottlich M, Munte TF, Heldmann M, Kasten M, Hagenah J, Kramer UM. Altered resting state brain networks in Parkinson's disease. PLoS One. 2013;8(10):77336.

10. Baggio HC, Sala-Llonch R, Segura B, et al. Functional brain networks and cognitive deficits in Parkinson's disease. Hum Brain Mapp. 2014;35(9):4620-34.

11. Skidmore F, Korenkevych D, Liu Y, He G, Bullmore E, Pardalos PM. Connectivity brain networks based on wavelet correlation analysis in Parkinson fMRI data. Neurosci Lett. 2011;499(1):47-51.

12. Gibb WR, Lees AJ. The relevance of the Lewy body to the pathogenesis of idiopathic Parkinson's disease. J Neurol Neurosurg Psychiatry. 1988;51(6):745-52.

13. Goetz CG, Tilley BC, Shaftman SR, et al. Movement Disorder Society-sponsored revision of the Unified Parkinson's Disease Rating Scale (MDS-UPDRS): scale presentation and clinimetric testing results. Mov Disord. 2008;23(15):2129-70.

14. Hoehn MM, Yahr MD. Parkinsonism: onset, progression and mortality. Neurology. 1967;17(5):427-42.

15. Folstein MF, Robins LN, Helzer JE. The Mini-Mental State Examination. Arch Gen Psychiatry. 1983;40(7):812.

16. Fox MD, Zhang D, Snyder AZ, Raichle ME. The global signal and observed anticorrelated resting state brain networks. J Neurophysiol. 2009;101(6):3270-83.

17. Wang J, Wang X, Xia M, Liao X, Evans A, He Y. GRETNA: a graph theoretical network analysis toolbox for imaging connectomics. Front Hum Neurosci. 2015;9:386.

18. Watts DJ, Strogatz SH. Collective dynamics of 'small-world' networks. Nature. 1998;393(6684):440-2.

19. Latora V, Marchiori M. Efficient behavior of small-world networks. Phys Rev Lett. 2001;87(19):198701.

20. Achard S, Bullmore E. Efficiency and cost of economical brain functional networks. PLoS Comput Biol. 2007;3(2):e17.

21. Zalesky A, Fornito A, Bullmore ET. Network-based statistic: identifying differences in brain networks. Neuroimage. 2010;53(4):1197-207.

22. Bullmore ET, Suckling J, Overmeyer S, Rabe-Hesketh S, Taylor E, Brammer MJ. Global, voxel, and cluster tests, by theory and permutation, for a difference between two groups of structural MR images of the brain. IEEE Trans Med Imaging. 1999;18(1):32-42.

23. BLINDED FOR REVIEW. Suo X, Lei D, Li K, et al. Disrupted brain network topology in pediatric posttraumatic stress disorder: A resting-state fMRI study. Hum Brain Mapp. 2015;36(9):3677-86.

24. BLINDED FOR REVIEW. Lei D, Li K, Li L, et al. Disrupted Functional Brain Connectome in Patients with Posttraumatic Stress Disorder. Radiology. 2015;276(3):818-27.

25. Benjamini Y, Drai D, Elmer G, Kafkafi N, Golani I. Controlling the false discovery rate in behavior genetics research. Behav Brain Res. 2001;125(1-2):279-84.

26. Sporns O, Tononi G, Kotter R. The human connectome: A structural description of the human brain. PLoS Comput Biol. 2005;1(4):e42.

27. Ma Q, Huang B, Wang J, et al. Altered modular organization of intrinsic brain functional networks in patients with Parkinson's disease. Brain Imaging Behav. 2017;11(2):430-43.

28. Galantucci S, Agosta F, Stefanova E, et al. Structural Brain Connectome and Cognitive Impairment in Parkinson Disease. Radiology. 2017;283(2):515-25.

29. Olde Dubbelink KT, Hillebrand A, Stoffers D, et al. Disrupted brain network topology in Parkinson's disease: a longitudinal magnetoencephalography study. Brain. 2014;137(Pt 1):197-207.

30. Liang P, Deshpande G, Zhao S, Liu J, Hu X, Li K. Altered directional connectivity between emotion network and motor network in Parkinson's disease with depression. Medicine (Baltimore). 2016;95(30):e4222.

31. Aarabi MH, Kamalian A, Mohajer B, et al. A statistical approach in human brain connectome of Parkinson Disease in elderly people using Network Based Statistics. Conf Proc IEEE Eng Med Biol Soc. 2015;2015:4310-3.

32. Meppelink AM, de Jong BM, Renken R, Leenders KL, Cornelissen FW, van Laar T. Impaired visual processing preceding image recognition in Parkinson’s disease patients with visual hallucinations. Brain. 2009;132(Pt 11):2980-93.

33. Raichle ME, MacLeod AM, Snyder AZ, Powers WJ, Gusnard DA, Shulman GL. A default mode of brain function. Proc Natl Acad Sci U S A. 2001;98(2):676-82.

34. Agosta F, Pievani M, Geroldi C, Copetti M, Frisoni GB, Filippi M. Resting state fMRI in Alzheimer’s disease: beyond the default mode network. Neurobiol Aging. 2012;33(8):1564-78.

35. Tessitore A, Esposito F, Vitale C, et al. Default-mode network connectivity in cognitively unimpaired patients with Parkinson disease. Neurology. 2012;79(23):2226-32.

36. Luo C, Guo X, Song W, et al. The trajectory of disturbed resting-state cerebral function in Parkinson's disease at different Hoehn and Yahr stages. Hum Brain Mapp. 2015;36(8):3104-16.

37. Olde Dubbelink KT, Stoffers D, Deijen JB, et al. Resting-state functional connectivity as a marker of disease progression in Parkinson's disease: A longitudinal MEG study. Neuroimage Clin. 2013;2:612-9.

38. Alafuzoff I, Ince PG, Arzberger T, et al. Staging/typing of Lewy body related alpha-synuclein pathology: a study of the BrainNet Europe Consortium. Acta Neuropathol. 2009;117(6):635-52.

39. Wu T, Long X, Zang Y, et al. Regional homogeneity changes in patients with Parkinson's disease. Hum Brain Mapp. 2009;30(5):1502-10.

40. New AB, Robin DA, Parkinson AL, et al. The intrinsic resting state voice network in Parkinson's disease. Hum Brain Mapp. 2015;36(5):1951-62.

Table 1. Demographics and clinical characteristics of the PD patients and healthy controls.

	HC	PD overall	H&Y stage 1	H&Y stage 1.5	H&Y stage 2	H&Y stage 2.5	H&Y stage 3	H&Y stage 4	P
Number	81	153	19	20	31	30	25	28	-
Age (y)	53.7±8.0 (36-70)	55.7±7.7 (35-71)	57.0±6.6 (42-70)	53.9±7.8 (41-67)	54.9±6.6 (42-65)	53.9±7.4 (35-63)	55.5±8.8 (38-71)	58.6±8.1 (40-69)	0.074[a], 0.115[b]
Gender (F/M)	45/36	86/67	10/9	15/5	14/17	13/17	16/9	18/10	0.516[c],0.163[d]
Education (y)	10.1±3.2 (5-16)	8.5±3.9 (0-18)	9.0±3.8 (0-15)	8.9±4.2 (0-17)	9.7±3.9 (1-16)	7.3±3.7 (1-13)	7.6±3.8 (1-18)	7.9±3.9 (0-16)	0.003[a], 0.117[b]
Disease duration(y)	NA	5.5±4.5 (0.2-22)	1.7±1.5 (0.2-6)	2.3±2.3 (0.3-8)	3.6±3.1 (0.5-12)	5.3±3.9 (1-13)	6.9±2.9 (2-12)	11.3±4.0 (6-22)	<0.001[b]
UPDRS III score	NA	27.8±15.5 (2-79)	11.3±4.8 (4-23)	14.4±5.5 (2-23)	21.5±8.2 (9-37)	31.4±12.0 (5-59)	40.6±8.9 (23-55)	45.4±14.1 (11-79)	<0.001[b]
MMSE score	NA	27.0±2.9 (18-30)	27.7±2.5 (21-30)	27.8±2.4 (23-30)	27.8±2.2 (21-30)	27.0±2.5 (21-30)	26.1±3.4 (18-30)	25.8±3.9 (18-30)	0.052[b]
Age at onset (y)	NA	50.3±8.4 (29-65)	55.4±6.9 (39-65)	51.2±9.0 (38-65)	51.1±7.2 (37-64)	49.0±7.8 (33-62)	48.8±9.5 (29-61)	47.8±8.5 (29-58)	0.040[b]
Side of onset (L/R/S)	NA	68/80/5	9/10/0	9/11/0	14/13/4	11/18/1	12/13/0	13/15/0	0.204[d]
Motor phenotype (T/A/M)	NA	65/60/28	9/8/2	7/7/6	15/12/4	9/12/9	13/8/4	12/13/3	0.540[d]
LEDD	NA	787.7±407.9 (75-2100)	515± 479 (112.5-1300)	416.2±364.9 (125-1100)	678.9±284.7 (300-1248)	692.5±304.9 (75-1165)	848.5±387.9 (350-2000)	1049.2±393 (425-2100)	<0.001[b]

Measurements presented as mean±SD with ranges in parentheses or number.

[a]p Values for comparisons between all PD and control participants using independent-sample t tests.

[b]p Values for comparisons among different H&Y stage PD using one-way analysis of variance.

[c]p Values obtained using chi-squared test between all PD and control participants.

[d]p Values obtained using chi-squared test among different H&Y stage PD.

Abbreviations: PD, Parkinson's disease; HC, healthy controls; H&Y, Hoehn and Yahr; y, years; F, female; M, male; L, left; R, right; S, symmetric; T, tremor-dominant; A, akinetic–rigid; M, mixed; UPDRS, Unified PD Rating Scale; MMSE, Mini–Mental State Examination; LEDD, levodopa equivalent daily dose; NA, not applicable.

Table 2. Regions showing decreased AUC values of nodal centralities in the PD group compared with HC.

	Nodal Degree			Nodal Efficiency			Nodal Betweenness		
Brain regions	PD	HC	P	PD	HC	P	PD	HC	P
Right PreCG	2.426±1.210 (0.159-6.071)	3.052±1.310 (0.051-5.805)	**0.0004**	0.071±0.012 (0.027-0.106)	0.078±0.014 (0.011-0.104)	**0.0002**	11.244±11.319 (0-74.780)	12.916±12.139 (0.045-65.520)	0.3023
Left SFG	2.336±1.247 (0.297-5.788)	2.774±1.159 (0.658-5.593)	0.0120	0.071±0.012 (0.040-0.104)	0.076±0.011 (0.055-0.102)	**0.0010**	9.768±10.093 (0-56.405)	11.703±9.904 (0.355-48.345)	0.1606
Right ROL	2.954±1.108 (0.795-6.312)	3.591±1.155 (1.141-6.341)	**0.0002**	0.076±0.010 (0.053-0.105)	0.083±0.010 (0.061-0.105)	**0.0002**	13.945±10.435 (0.215-58.965)	15.909±10.966 (0.335-53.235)	0.1850
Right PCG	2.146±1.279 (0.158-5.726)	2.721±1.443 (0.340-6.133)	0.0030	0.068±0.013 (0.032-0.103)	0.075±0.014 (0.042-0.108)	**0.0002**	8.456±10.266 (0-69.300)	10.276±11.944 (0-57.600)	0.2254
Right FFG	2.615±1.312 (0.258-6.496)	3.335±1.340 (0.807-6.881)	**0.0002**	0.072±0.013 (0.037-0.107)	0.079±0.014 (0.047-0.113)	**0.0002**	12.553±11.722 (0.010-69.665)	15.009±13.258 (0-71.000)	0.1516
Left PoCG	2.539±1.311 (0.123-6.513)	3.255±1.460 (0.837-6.967)	**0.0002**	0.072±0.013 (0.027-0.106)	0.080±0.014 (0.054-0.112)	**0.0002**	12.859±13.468 (0-84.420)	14.462±12.256 (0.130-57.615)	0.3787
Right PoCG	2.645±1.399 (0.385-6.269)	3.498±1.480 (1.025-7.351)	**0.0002**	0.073±0.014 (0.037-0.104)	0.082±0.014 (0.054-0.115)	**0.0002**	12.892±12.292 (0.315-74.520)	18.838±17.808 (0.370-80.565)	0.0028
Right SMG	2.639±1.381 (0.372-7.333)	3.135±1.304 (0.365-6.875)	0.0084	0.073±0.013 (0.046-0.111)	0.079±0.012 (0.042-0.109)	**0.0010**	13.396±12.316 (0-63.860)	16.615±12.850 (0.080-60.015)	0.0660
Left ANG	2.622±1.261 (0.327-5.821)	3.217±1.334 (0.333-7.040)	**0.0010**	0.073±0.012 (0.038-0.102)	0.079±0.012 (0.041-0.113)	**0.0002**	15.006±11.382 (0.125-66.340)	20.180±17.246 (0.205-77.710)	0.0052
Left HES	2.093±0.994 (0.218-4.529)	2.526±1.095 (0.291-4.892)	0.0028	0.068±0.011 (0.032-0.092)	0.074±0.011 (0.040-0.097)	**0.0006**	5.265±6.082 (0-30.340)	5.489±7.154 (0-40.610)	0.8054
Left STG	2.969±1.129 (0.879-5.886)	3.387±1.088 (0.426-5.776)	0.0078	0.076±0.011 (0.052-0.104)	0.082±0.010 (0.045-0.104)	**0.0010**	14.998±11.673 (0.315-57.325)	15.140±12.282 (0.035-62.068)	0.9302
Right STG	2.554±1.131 (0.275-6.126)	3.003±1.196 (0.090-6.228)	0.0062	0.072±0.011 (0.046-0.104)	0.078±0.011 (0.032-0.105)	**0.0008**	10.797±8.552 (0-41.805)	11.068±9.976 (0-37.775)	0.8310

Measurements presented as mean±SD with ranges in parentheses.

Regions were considered abnormal in the PD patients if they exhibited significant between-group differences ($P < 0.001$, FDR corrected) in at least one of the three nodal centralities (P shown in bold font). Abbreviations: AUC, area under the curve; PD, Parkinson's disease; HC, healthy control; PreCG, precentral gyrus; SFG, superior frontal gyrus; ROL, rolandic operculum; PCG, posterior cingulate gyrus; FFG, fusiform gyrus; PoCG, postcentral gyrus; SMG, supramarginal gyrus; ANG, angular gyrus; HES, Heschl gyrus; STG, superior temporal gyrus.

Table 3. T values of functional connections between the brain regions showing decreased nodal centralities trend with increasing Hoehn and Yahr stage and the default mode network regions.

Regions	Right PCG	Left SFG	Left ANG
Right PreCG	4.27	3.48	3.65
Left PoCG	1.94	1.94	2.60
Left STG	3.16	4.68	4.82

The nodal centralities in the right PreCG, left PoCG and left STG had a tendency to decrease with increase in Hoehn and Yahr stage as shown in Figure 3. In the network-based statistics, the above three brain regions were all connected with default mode network regions including right PCG, left SFG and left ANG ($P < 0.05$). See Figure 2 for a graphical presentation of these connections. Table 3 shows the T values of these connections. PreCG, precentral gyrus; PoCG, postcentral gyrus; STG, superior temporal gyrus; PCG, posterior cingulate gyrus; SFG, superior frontal gyrus; ANG, angular gyrus.

Figure 1. The differences in topological properties of the brain functional connectome between PD patients and HC. PD patients showed significantly decreased Eglobal (P = 0.0002), Elocal (P = 0.0006), and Cp (P = 0.0002), and increased Lp (P = 0.0006). PD, Parkinson's disease; HC, healthy control; Eglobal, global efficiency; Elocal, local efficiency; Cp, clustering coefficient; Lp, characteristic path length.

Figure 2. Significantly decreased nodal centralities (nodes shown in light blue) of the brain functional connectome in PD patients. These connections formed a single connected network with 12 nodes and 28 connections (P < 0.05, network-based statistics). All connections exhibited decreased values in the PD. Decreased nodal centralities in the right PreCG, left PoCG and left STG (nodes shown in dark blue) with increasing Hoehn and Yahr stage in PD, which were all connected with left ANG, left SFG and right PCG. PD, Parkinson's disease; R, right; L, left; PreCG, precentral gyrus; ROL, rolandic operculum; PCG, posterior cingulate gyrus; FFG, fusiform gyrus; SMG, supramarginal gyrus; PoCG, postcentral gyrus; SFG, superior frontal gyrus; ANG, angular gyrus; HES, Heschl gyrus; STG, superior temporal gyrus.

Figure 3. The brain regions showing decreased nodal centralities trend with increasing Hoehn and Yahr stage. Decreased trend of the nodal centralities in the right PreCG, left PoCG and left STG as the increasing Hoehn and Yahr stage in the PD patients. PD, Parkinson's disease; R, right; L, left; PreCG, precentral gyrus; PoCG, postcentral gyrus; STG, superior temporal gyrus. * represent P < 0.05, with one-way analysis of variance followed by post hoc two-sample t tests.

Figure 4. Correlation between the brain regions showing decreased nodal centralities trend with increasing Hoehn and Yahr stage and UPDRS-III in PD patients. UPDRS-III score was negatively correlated with nodal degree of the left PoCG and nodal efficiency of left STG. PD, Parkinson's disease; UPDRS, Unified PD Rating Scale; L, left; PoCG, postcentral gyrus; STG, superior temporal gyrus.